Article

Solid-State Ru-99 NMR Spectroscopy: A Useful Tool for Characterizing Prototypal Diamagnetic Ruthenium Compounds

Kristopher J. Ooms, and Roderick E. Wasylishen

J. Am. Chem. Soc., **2004**, 126 (35), 10972-10980• DOI: 10.1021/ja0400887 • Publication Date (Web): 11 August 2004

J|A|C|S
ARTICLES
Published on Web 08/11/2004

Solid-State Ru-99 NMR Spectroscopy: A Useful Tool for Characterizing Prototypal Diamagnetic Ruthenium Compounds

Kristopher J. Ooms and Roderick E. Wasylishen*

Contribution from the Department of Chemistry, University of Alberta, Edmonton, Alberta, T6G 2G2, Canada

Received March 26, 2004; Revised Manuscript Received June 16, 2004; E-mail: roderick.wasylishen@ualberta.ca

Abstract: The feasibility of ^{99}Ru NMR spectroscopy as a tool to characterize solid compounds is demonstrated. Results of the first solid-state ^{99}Ru NMR investigation of diamagnetic compounds are presented for $Ru(NH_3)_6Cl_2$, $K_4Ru(CN)_6 \cdot xH_2O$ ($x = 0$, 3), $LaKRu(CN)_6$, and $Ru_3(CO)_{12}$. The sensitivity of the ruthenium magnetic shielding tensor to subtle changes in the local structure about the ruthenium nucleus is highlighted by comparing the ^{99}Ru isotropic chemical shift of $Ru(NH_3)_6Cl_2$ in aqueous solutions and in the solid state. The narrow isotropic ^{99}Ru NMR peak observed for solid $Ru(NH_3)_6Cl_2$ indicates that this compound is an ideal secondary reference sample for solid-state ^{99}Ru NMR studies. The isotropic ^{99}Ru chemical shift, ^{99}Ru nuclear quadrupolar coupling constant, C_Q, and quadrupolar asymmetry parameter of $K_4Ru(CN)_6 \cdot xH_2O$ ($x = 0$, 3) are shown to be sensitive to x. For $Ru_3(CO)_{12}$, the magnetic shielding tensors of each of the three nonequivalent Ru nuclei have spans of 1300−1400 ppm, and the ^{99}Ru C_Q values are also similar, 1.36−1.85 MHz, and are surprisingly small given that ^{99}Ru has a moderate nuclear quadrupole moment. Information about the relative orientation of the Ru magnetic shielding and electric field gradient tensors has been determined for $Ru_3(CO)_{12}$ from experimental ^{99}Ru NMR spectra as well as quantum chemical calculations.

Introduction

Despite the importance of ruthenium in modern chemistry,[1−3] the study of ruthenium by nuclear magnetic resonance (NMR) spectroscopy has been limited because of its unfavorable nuclear properties. Ruthenium has two NMR-active isotopes, ^{99}Ru and ^{101}Ru, both of which may be classified as "low-gamma" nuclei, i.e., they have magnetogyric ratios (γ) less than that of ^{15}N ($\gamma(^{99}Ru) = -1.229 \times 10^7$ rad s^{-1} T^{-1}, $\Xi(^{99}Ru) = 4.605$ MHz; $\gamma(^{101}Ru) = -1.377 \times 10^7$ rad s^{-1} T^{-1}, $\Xi(^{101}Ru) = 5.161$ MHz).[4,5] To further complicate matters, both ^{99}Ru and ^{101}Ru have low natural abundances, 12.76 and 17.06%, respectively, are quadrupolar nuclei with nuclear spins of 5/2, and have moderate and large nuclear quadrupole moments ($Q(^{99}Ru) = 7.9$ fm^2, $Q(^{101}Ru) = 45.7$ fm^2).[5] Although the relative NMR receptivity of ^{101}Ru is approximately 1.9 times greater than that of ^{99}Ru, the latter isotope is preferred for ruthenium NMR because of its smaller nuclear quadrupole moment.

While more than 20 years have passed since the first reported solution ^{99}Ru NMR investigation,[6] such studies are limited;[7,8] to our knowledge there have been only 16 ^{99}Ru NMR papers published, encompassing approximately 100 different ruthenium compounds.[6,9−23] These studies have established that the chemical shift (CS) range of ruthenium is approximately 18 000 ppm, with $\delta_{iso} = +16050$ ppm and -1338 ppm for $Ru(OH_2)_6^{2+}$ and $[RuCp(CO)_2]_2$, respectively, relative to solutions of $K_4Ru(CN)_6$.[22,23] The large CS range of ruthenium is comparable to that of cobalt, which is generally acknowledged as having one

(1) Keefe, M. H.; Benkstein, K. D.; Hupp, J. T. *Coord. Chem. Rev.* **2000**, *205*, 201−228.
(2) Naota, T.; Takaya, H.; Murahashi, S. *Chem. Rev.* **1998**, *98*, 2599−2660.
(3) Coville, N. J.; Cheng, L. *J. Organomet. Chem.* **1998**, *571*, 149−169.
(4) Smith, M. E.; van Eck, E. R. H. *Prog. Nucl. Magn. Reson. Spectrosc.* **1999**, *34*, 159−201.
(5) Harris, R. K.; Becker, E. D.; De Menezes, S. M. C.; Goodfellow, R.; Granger, P. *Pure Appl. Chem.* **2001**, *73*, 1795−1818.
(6) Brevard, C.; Granger, P. *J. Chem. Phys.* **1981**, *75*, 4175−4177.
(7) Granger, P. In *Encyclopedia of Nuclear Magnetic Resonance*; Grant, D. M., Harris, R. K., Eds.; John Wiley & Sons: Chichester, 2002; Vol. 6, pp 3889−3900.
(8) Goodfellow, R. In *Multinuclear NMR*; Mason, J., Ed.; Plenum: New York, 1989; pp 521−561.
(9) Dykstra, R. W.; Harrison, A. M. *J. Magn. Reson.* **1982**, *46*, 338−342.
(10) Brevard, C.; Granger, P. *Inorg. Chem.* **1983**, *22*, 532−535.
(11) Steel, P. J.; LaHousse, F.; Lerner, D.; Marzin, C. *Inorg. Chem.* **1983**, *22*, 1488−1493.
(12) Bernhard, P.; Helm, L.; Rapaport, I.; Ludi, A.; Merbach, A. E. *Chem. Commun.* **1984**, 302−303.
(13) Marzin, C.; Budde, F.; Steel, P. J.; Lerner, D. *Nouv. J. Chim.* **1987**, *11*, 33−41.
(14) Orellana, G.; Kirsch-De Mesmaeker, A.; Turro, N. J. *Inorg. Chem.* **1990**, *29*, 882−885.
(15) Braunstein, P.; Rosé, J.; Granger, P.; Richert, T. *Magn. Reson. Chem.* **1991**, *29*, S31−S37.
(16) Emelyanov, V. A.; Fedotov, M. A.; Belyaev, A. V. *Zh. Neorg. Khim.* **1993**, *38*, 1842−1848.
(17) Predieri, G.; Vignali, C.; Denti, G.; Serroni, S. *Inorg. Chim. Acta* **1993**, *205*, 145−148.
(18) Granger, P.; Richert, T.; Elbayed, K.; Kempgens, P.; Hirschinger, J.; Raya, J.; Rosé, J.; Braunstein, P. *Mol. Phys.* **1997**, *92*, 895−902.
(19) Xiao, X. M.; Matsumura-Inoue, T.; Mizutani, S. *Chem. Lett.* **1997**, 241−242.
(20) Ferrari, M. B.; Fava, G. G.; Pelosi, G.; Predieri, G.; Vignali, C.; Denti, G.; Serroni, S. *Inorg. Chim. Acta* **1998**, *276*, 320−326.
(21) Xiao, X. M.; Matsumura-Inoue, T. *Chin. Chem. Lett.* **1998**, *9*, 765−766.
(22) Gaemers, S.; van Slageren, J.; O'Connor, C. M.; Vos, J. G.; Hage, R.; Elsevier, C. J. *Organometallics* **1999**, *18*, 5238−5244.
(23) Bernhard, P.; Helm, L.; Ludi, A.; Merbach, A. E. *J. Am. Chem. Soc.* **1985**, *107*, 312−317.

10.1021/ja0400887 CCC: $27.50

of the largest CS ranges of all nuclei in the NMR periodic table.[7,8] Two computational studies have also been reported to investigate the reliability of current computational methods in calculating ^{99}Ru NMR isotropic chemical shifts.[24,25]

There have been no reports of $^{99/101}$Ru NMR studies of nonmetallic diamagnetic ruthenium compounds in the solid state, i.e., where ruthenium is in either the 0, +2, or +8 oxidation state. A number of ^{99}Ru and ^{101}Ru solid-state NMR and nuclear quadrupolar resonance (NQR) studies have been published for metallic, paramagnetic, ferromagnetic, and superconducting ruthenium compounds.[26−40] The absence of $^{99/101}$Ru NMR data for solid diamagnetic compounds can be appreciated if it is recognized that the NMR receptivity of ^{99}Ru is 1400 times less than that of ^{27}Al; thus, assuming the same peak widths and relaxation times, a ^{99}Ru NMR spectrum would take approximately two million times longer to acquire than a comparable quality ^{27}Al NMR spectrum.[5]

Both the magnetic shielding (σ) and electric field gradient (EFG) are second-rank tensors; thus, they contain both magnitude and orientational information.[41−45] In isotropic solutions, rapid molecular tumbling results in averaging of the magnetic shielding and EFG tensors, and all orientational information is lost. In contrast, in the solid-state experimentalists have an opportunity to probe the orientational dependence of these interactions.

We present ^{99}Ru NMR spectra using magic-angle spinning (MAS) and stationary samples of solid $Ru(NH_3)_6Cl_2$, $K_4Ru(CN)_6 \cdot xH_2O$ (x = 0, 3), $LaKRu(CN)_6$, and $Ru_3(CO)_{12}$. To complement the experimental results, quantum chemical density functional theory (DFT) computations using hybrid functionals are presented.

Experimental Section

(a) Materials. $Ru(NH_3)_6Cl_2$, $K_4Ru(CN)_6 \cdot 3H_2O$, and $Ru_3(CO)_{12}$ were obtained from Strem Chemicals, Inc. and used without further purification. $LaKRu(CN)_6 \cdot 4H_2O$ was prepared according to literature methods.[46] Powder X-ray diffraction measurements indicated that trace amounts of $K_4Ru(CN)_6 \cdot 3H_2O$ were present in the $LaKRu(CN)_6 \cdot 4H_2O$ sample; however, the impurity did not interfere with the NMR analysis as their respective ^{99}Ru NMR chemical shifts are different.

(b) NMR Spectroscopy. Solid-state ^{99}Ru NMR spectra were acquired on a Bruker Avance 500 and a Varian Inova 750 spectrometer operating at 23.040 MHz (B_0 = 11.75 T) and 34.516 MHz (B_0 = 17.6 T), respectively. Ruthenium chemical shifts were referenced using a 0.3 M solution of $K_4Ru(CN)_6$ in D_2O at 20 ± 1 °C, δ_{iso} = 0.0 ppm and $\Xi(^{99}Ru)$ = 4.605151 MHz.[5] This sample was also used to determine 90° pulse widths of 9.75 μs ($\gamma B_1/2\pi$ = 25.6 kHz) and 12.0 μs ($\gamma B_1/2\pi$ = 20.8 kHz) at 11.75 and 17.6 T, respectively. The magic angle was set by maximizing the number of rotational echoes observed in the ^{35}Cl NMR free-induction decay of solid NaCl or those of the ^{79}Br NMR signal of KBr.[47] At 11.75 T, a wide-bore (89 mm) Bruker double resonance probe (7 mm O. D. rotor) was used to obtain spectra with MAS. Spinning rates ranged from 2.0 to 7.0 kHz, and were controlled by an automated MAS pneumatic control unit to better than 2 Hz stability. A home-built MAS probe (5 mm O. D. rotor) was used to obtain MAS rates up to 9.0 kHz on the Varian 750 spectrometer (51 mm bore magnet). All MAS spectra were acquired using a one-pulse sequence. Because of extensive probe ringing at these low frequencies, dead times of approximately 100 μs at 11.75 T and 150 μs at 17.6 T were necessary. The pulse length used at 11.75 T for solid samples was 3.25 μs, which corresponds to a 30° nonselective "solution" pulse. At 17.6 T a 22.5° pulse was used (τ_p = 3.0 μs) to allow for slightly shorter recycle delays and a broader excitation envelope. Recycle delays ranged from 2 to 4 s. The quadrupolar Carr−Purcell Meiboom−Gill (QCPMG) pulse sequence was used and has proven to be useful in obtaining sensitivity enhancements in NMR spectra of stationary samples for quadrupolar nuclei with low receptivities.[48,49] Echo delays in the QCPMG experiment were 128 μs, and the excitation and refocusing pulse lengths were 3.25 and 6.50 μs, respectively, at 11.75 T. Proton decoupling was used for $Ru(NH_3)_6Cl_2$, employing a decoupling field strength of approximately 42 kHz. For the hydrates of the ruthenium(II) hexacyanides, use of ^{1}H decoupling resulted in no noticeable line-narrowing under MAS conditions.

All ^{99}Ru NMR spectra, including those acquired on the Inova 750, were processed using the Bruker software, WINNMR. Gaussian line-broadening functions of 20−200 Hz were applied to the free-induction decays prior to Fourier transformation. Spectra were simulated using CSOLIDS,[50] a program developed in this lab, and SIMPSON.[51] For $Ru_3(CO)_{12}$, the three ruthenium sites were simulated independently, and the resulting spectra were co-added using WINNMR.

(c) Computations. Calculations of the ruthenium magnetic shielding tensors were performed using Gaussian 98W (revision A.7)[52] and the NMR module[53−57] of the Amsterdam Density Functional (ADF 2002.02) package.[17,58] B3LYP[59,60] calculations were performed on a Windows-based Intel PC using the DZVP local spin density basis set (6s5p3d)[61] for ruthenium and the 6-31G(d) basis sets for all other atoms, as available in the Gaussian package. While it is recognized that the DZVP basis set for Ru is small, higher level computations were not possible

(24) Bühl, M.; Gaemers, S.; Elsevier: C. J. *Chem.−Eur. J.* **2000**, *6*, 3272−3280.
(25) Bagno, A.; Bonchio, M. *Eur. J. Inorg. Chem.* **2002**, 1475−1483.
(26) Kumagai, K.; Takada, S.; Furukawa, Y. *Hyperfine Interact.* **2001**, *133*, 151−156.
(27) Ishida, K.; Mukuda, H.; Kitaoka, Y.; Mao, Z. Q.; Fukazawa, A.; Maeno, Y. *J. Magn. Magn. Mater.* **2001**, *226*, 353−354.
(28) Tokunaga, Y.; Kotegawa, H.; Ishida, K.; Kitaoka, Y.; Takagiwa, H.; Akimitsu, J. *Phys. Rev. Lett.* **2001**, *86*, 5767−5770.
(29) Kumagai, K.; Takada, S.; Furukawa, Y. *Phys. Rev. B* **2001**, *63*, 180509.
(30) Ishida, K.; Mukuda, H.; Kitaoka, Y.; Mao, Z. Q.; Fukazawa, H.; Maeno, Y. *Phys. Rev. B* **2001**, *63*, 060507.
(31) Mukuda, H.; Ishida, K.; Kitaoka, Y.; Kanno, R.; Takano, M. *Physica B* **2000**, *284*, 1467−1468.
(32) Matsuda, K.; Kohori, Y.; Kohara, T.; Fujiwara, K. *J. Phys.: Condens. Matter.* **2000**, *12*, 2061−2069.
(33) Mukuda, H.; Ishida, K.; Kitaoka, Y.; Asayama, K.; Kanno, R.; Takano, M. *Phys. Rev. B* **1999**, *60*, 12279−12285.
(34) Kawasaki, Y.; Ishida, K.; Kitaoka, Y.; Asayama, K.; Nakamura, H.; Flouquet, J. *Physica B* **1999**, *261*, 77−78.
(35) Ishida, K.; Kawasaki, Y.; Kitaoka, Y.; Asayama, K.; Nakamura, H.; Flouquet, J. *Phys. Rev. B* **1998**, *57*, R11054−R11057.
(36) Ishida, K.; Kitaoka, Y.; Asayama, K.; Ikeda, S.; Nishizaki, S.; Maeno, Y.; Yoshida, K.; Fujita, T. *Phys. Rev. B* **1997**, *56*, R505−R508.
(37) Ishida, K.; Kitaoka, Y.; Asayama, K.; Ikeda, S.; Maeno, Y.; Fujita, T. *Czech. J. Phys.* **1996**, *46*, 1093−1094.
(38) Ishida, K.; Mukuda, H.; Kitaoka, Y.; Asayama, K.; Onuki, Y. *Z. Naturforsch., A: Phys. Sci.* **1996**, *51*, 793−796.
(39) Burgstaller, A.; Ebert, H.; Voitländer, J. *Hyperfine Interact.* **1993**, *80*, 1015−1018.
(40) Burgstaller, A.; Voitländer, J.; Ebert, H. *J. Phys.: Condens. Matter.* **1994**, *6*, 8335−8340.
(41) Mehring, M. *Principles of High-Resolution NMR in Solids*; Springer-Verlag: New York, 1983.
(42) MacKenzie, K. J. D.; Smith, M. E. *Multinuclear Solid-State NMR of Inorganic Materials*; Pergamon: Oxford, 2002; Vol. 6.
(43) Levitt, M. H. *Spin Dynamics: Basics of Nuclear Magnetic Resonance*; John Wiley & Sons: Chichester, New York, 2001.
(44) Haeberlen, U. *Advances in Magnetic Resonance, Supplement 1*; Waugh, J. S., Ed; Academic Press: New York, 1976.
(45) *Solid-State NMR Spectroscopy: principles and applications*; Duer, M., Ed.; Blackwell Science: Oxford, 2002.
(46) Mullica, D. F.; Hayward, P. K.; Sappenfield, E. L. *Inorg. Chim. Acta* **1996**, *244*, 273−276.
(47) Frye, J. S.; Maciel, G. E. *J. Magn. Reson.* **1982**, *48*, 125−131.
(48) Larsen, F. H.; Jakobsen, H. J.; Ellis, P. D.; Nielsen, N. C. *J. Magn. Reson.* **1998**, *131*, 144−147.
(49) Larsen, F. H.; Jakobsen, H. J.; Ellis, P. D.; Nielsen, N. C. *J. Phys. Chem. A* **1997**, *101*, 8597−8606.
(50) Eichele, K.; Wasylishen, R. E. *Csolids*, version 1.4.12; University of Alberta, 2002.
(51) Bak, M.; Rasmussen, J. T.; Nielsen, N. C. *J. Magn. Reson.* **2000**, *147*, 296−330.

with the computer resources currently available to us.[24] ADF calculations were performed on an 8-processor AMD-based Linux cluster using the zeroth-order regular approximation (ZORA) TZ2P basis sets (valence triple-ζ, doubly polarized), and they included scalar and spin−orbit relativistic corrections. The exchange-correlation functional employed the LDA of Vosko, Wilk, Nusair (VWN)[62] and the GGA of Becke88[63] and Perdew86.[64,65] The atomic coordinates of $Ru_3(CO)_{12}$ were calculated from the X-ray crystal structure determined by Churchill et al.[66] The calculated principal components of the magnetic shielding tensor, σ_{ii} ($i = 1$, 2, or 3), were converted to principal components of the chemical shift tensors, δ_{ii}, using the relation $\delta_{ii} = [(\sigma_{iso}(ref) - \sigma_{ii})]/[(1 - \sigma_{iso}(ref))]$, where $\sigma_{iso}(ref)$ is the calculated isotropic magnetic shielding of $K_4Ru(CN)_6$. This value was calculated using the geometry-optimized structure previously reported by Bühl et al. which includes the four potassium atoms.[24]

In assigning the principal components of the magnetic shielding tensor, we have followed the conventions summarized by Mason;[67] thus, $\sigma_{11} \leq \sigma_{22} \leq \sigma_{33}$ and $\delta_{11} \geq \delta_{22} \geq \delta_{33}$. The span of the magnetic shielding tensor is defined as:

$$\Omega = \sigma_{33} - \sigma_{11} = \delta_{11} - \delta_{33} \quad (1)$$

and the skew as:

$$\kappa = 3(\sigma_{iso} - \sigma_{22})/\Omega = 3(\delta_{22} - \delta_{iso})/\Omega \quad (2)$$

where $\sigma_{iso} = (\sigma_{11} + \sigma_{22} + \sigma_{33})/3$ and $\delta_{iso} = (\delta_{11} + \delta_{22} + \delta_{33})/3$.

Experimentally, the EFG tensor is generally characterized by the nuclear quadrupolar coupling constant, C_Q,

$$C_Q = eQV_{ZZ}/h \quad (3)$$

and the quadrupolar asymmetry parameter, η,

$$\eta_Q = (V_{XX} - V_{YY})/V_{ZZ} \quad (4)$$

where the principal components of the EFG tensor in its principal axis system (PAS) are defined such that $|V_{ZZ}| \geq |V_{YY}| \geq |V_{XX}|$.

The calculated principal components of the EFG tensor were converted from atomic units to Vm^{-2} by multiplying the values in au by 9.7177×10^{21} Vm^{-2}. The principal components of the EFG tensor were then expressed in terms of C_Q and η_Q.

Table 1. Experimental ^{99}Ru NMR Parameters Determined for the Hexaammine Ruthenium(II) Cation and Hexacyanoruthenate(II) Anion in Aqueous Solutions and the Solid State

compound	δ_{iso}/ppm	C_Q/MHz	η_Q
0.3 M $Ru(NH_3)_6Cl_2$ in H_2O	7750 ± 0.5		
saturated $Ru(NH_3)_6Cl_2$ in D_2O	7821[a]		
0.5 M $Ru(NH_3)_6Cl_2$ in D_2O	7680 ± 0.5		
0.3 M $Ru(NH_3)_6Cl_2$ in D_2O	7671 ± 3		
$Ru(NH_3)_6Cl_2$ solid	7569 ± 1	0	
0.3 M $K_4Ru(CN)_6$ in D_2O	0		
$LaKRu(CN)_6 \cdot 4H_2O$ solid	-247 ± 2	0	
$K_4Ru(CN)_6$ solid	17 ± 1	0.35 ± 0.02	0.85 ± 0.05
$K_4Ru(CN)_6 \cdot 3H_2O$ solid	-14 ± 1	0.40 ± 0.05	0.1 ± 0.1

[a] Value taken from ref 10.

The relative orientation of the EFG tensor and the magnetic shielding tensor are defined by three Euler angles (α, β, and γ), which are the counterclockwise rotations required to bring the PAS of the EFG tensor into coincidence with the PAS of the magnetic shielding tensor.[45]

Results and Discussion

(a) $Ru(NH_3)_6Cl_2$. Isotropic ^{99}Ru NMR chemical shift values for solid $Ru(NH_3)_6Cl_2$ and a number of aqueous solutions of $Ru(NH_3)_6Cl_2$ are presented in Table 1. From these data, it is clear that the ^{99}Ru chemical shift is sensitive to changes in the local environment. As the concentration of $Ru(NH_3)_6Cl_2$ in D_2O increases, δ_{iso} increases from 7671 ± 3 ppm for a 0.3 M solution to 7821 ppm for a saturated solution.[10] A similar but smaller concentration effect has been observed for the ^{59}Co chemical shift of $K_3Co(CN)_6$.[68] A large ^{2}H-isotope shift of 79 ppm to low frequency is observed when the solvent is changed from H_2O to D_2O, respectively. For $Co(NH_3)_6Cl_3$, the ^{2}H-isotope effect on the cobalt isotropic chemical shift is 94 ppm, with the cobalt also being more shielded in D_2O.[69]

$Ru(NH_3)_6Cl_2$ crystallizes in the cubic space group $Fm\bar{3}m$, which places Ru in a site of octahedral symmetry and dictates an isotropic magnetic shielding tensor ($\sigma_{11} = \sigma_{22} = \sigma_{33}$) and a null EFG ($V_{XX} = V_{YY} = V_{ZZ} = 0$).

The ^{99}Ru NMR spectrum of solid $Ru(NH_3)_6Cl_2$ obtained with MAS is presented in Figure 1a. The spectrum consists of one narrow isotropic peak at 7569 ± 1 ppm with a width at half-height, $\Delta\nu_{1/2}$, of 135 ± 20 Hz at 11.75 T. There is no evidence of magnetic shielding anisotropy or nuclear quadrupole interactions, as expected on the basis of the crystal structure. The ruthenium nucleus is 102 ppm more shielded in the solid state than in the 0.3 M solution of $Ru(NH_3)_6Cl_2$ in D_2O. A similar change in the ^{59}Co isotropic chemical shift occurs for $Co(NH_3)_6Cl_3$, where δ_{iso} increases when the solid is dissolved in an aqueous solution by 217, 281, and 332 ppm for the three unique cobalt sites.[70] Given the ^{2}H-isotope shift, this would yield changes of approximately 123, 187, and 238 ppm for a D_2O solution.

Since the narrow ^{99}Ru NMR peak for solid $Ru(NH_3)_6Cl_2$ is readily observed, we suggest that this compound be used as a secondary solid-state reference sample for ruthenium NMR studies ($\Xi(^{99}Ru) = 4.640\,007 \pm 0.000\,028$ MHz). The ^{99}Ru spin−lattice relaxation time, T_1, for this sample is approximately 1 s, determined using an inversion−recovery experiment, thus allowing for rapid signal acquisition. Under MAS conditions,

(52) Frisch, M. J.; Trucks, G. W.; Schlegel, H. B.; Scuseria, G. E.; Robb, M. A.; Cheeseman, J. R.; Zakrzewski, V. G.; Montgomery, J. A., Jr.; Stratmann, R. E.; Burant, J. C.; Dapprich, S.; Millam, J. M.; Daniels, A. D.; Kudin, K. N.; Strain, M. C.; Farkas, O.; Tomasi, J.; Barone, V.; Cossi, M.; Cammi, R.; Mennucci, B.; Pomelli, C.; Adamo, C.; Clifford, S.; Ochterski, J.; Petersson, G. A.; Ayala, P. Y.; Cui, Q.; Morokuma, K.; Malick, D. K.; Rabuck, A. D.; Raghavachari, K.; Foresman, J. B.; Cioslowski, J.; Ortiz, J. V.; Stefanov, B. B.; Liu, G.; Liashenko, A.; Piskorz, P.; Komaromi, I.; Gomperts, R.; Martin, R. L.; Fox, D. J.; Keith, T.; Al-Laham, M. A.; Peng, C. Y.; Nanayakkara, A.; Gonzalez, C.; Challacombe, M.; Gill, P. M. W.; Johnson, B. G.; Chen, W.; Wong, M. W.; Andres, J. L.; Head-Gordon, M.; Replogle, E. S.; Pople, J. A. *Gaussian 98*, revision A.7; Gaussian, Inc.: Pittsburgh, PA, 1998.
(53) Schreckenbach, G.; Ziegler, T. *J. Phys. Chem.* **1995**, *99*, 606−611.
(54) Schreckenbach, G.; Ziegler, T. *Int. J. Quantum Chem.* **1996**, *60*, 753−766.
(55) Schreckenbach, G.; Ziegler, T. *Int. J. Quantum Chem.* **1997**, *61*, 899−918.
(56) Wolff, S. K.; Ziegler, T. *J. Chem. Phys.* **1998**, *109*, 895−905.
(57) Wolff, S. K.; Ziegler, T.; van Lenthe, E.; Baerends, E. J. *J. Chem. Phys.* **1999**, *110*, 7689−7698.
(58) Guerra, C. F.; Snijders, J. G.; te Velde, G.; Baerends, E. J. *Theor. Chem. Acc.* **1998**, *99*, 391−403.
(59) Lee, C.; Yang, W.; Parr, R. G. *Phys. Rev. B* **1988**, *37*, 785.
(60) Becke, A. D. *J. Chem. Phys.* **1993**, *98*, 5648.
(61) Godbout, N.; Salahub, D. R.; Andzelm, J.; Wimmer, E. *Can. J. Chem.* **1992**, *70*, 560−571.
(62) Vosko, S. H.; Wilk, L.; Nusair, M. *Can. J. Phys.* **1980**, *58*, 1200−1211.
(63) Becke, A. D. *Phys. Rev. A* **1988**, *38*, 3098−3100.
(64) Perdew, J. P. *Phys. Rev. B* **1986**, *33*, 8822−8824.
(65) Perdew, J. P. *Phys. Rev. B* **1986**, *34*, 7406.
(66) Churchill, M. R.; Hollander, F. J.; Hutchinson, J. P. *Inorg. Chem.* **1977**, *16*, 2655−2659.
(67) Mason, J. *Solid State Nucl. Magn. Reson.* **1993**, *2*, 285−288.
(68) Ader, R.; Loewenstein, A. *J. Magn. Reson.* **1971**, *5*, 248.
(69) Bendall, M. R.; Doddrell, D. M. *Aust. J. Chem.* **1978**, *31*, 1141−1143.
(70) Medek, A.; Frydman, V.; Frydman, L. *J. Phys. Chem. B* **1997**, *101*, 8959−8966.

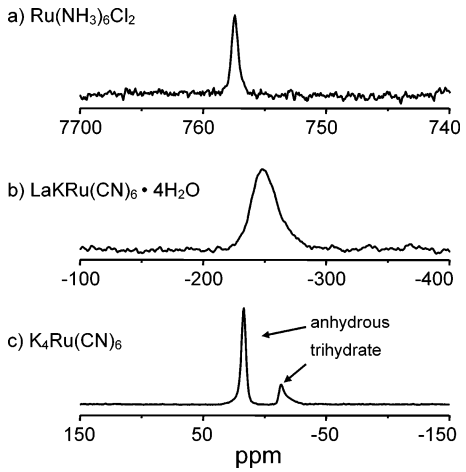

Figure 1. Solid-state ^{99}Ru NMR spectra of three Ru(II) compounds acquired at 23.040 MHz (11.75 T) with MAS. (a) $Ru(NH_3)_6Cl_2$; 2 k scans, 2 s recycle delay, MAS rate of 5.0 kHz. (b) $LaKRu(CN)_6 \cdot 4H_2O$; 80 k scans, 1 s recycle delay, MAS rate of 2.5 kHz. (c) Expansion of the central transition peaks ($^1/_2 \leftrightarrow -^1/_2$) for $K_4Ru(CN)_6 \cdot xH_2O$; 89 k scans, 0.5 s recycle delay, MAS rate of 6.5 kHz.

a signal-to-noise ratio of 5:1 can be achieved in 16 scans at 11.75 T using a 7 mm O. D. rotor, which makes solid $Ru(NH_3)_6Cl_2$ an ideal setup sample for ^{99}Ru NMR experiments.

(b) $LaKRu(CN)_6$ and $K_4Ru(CN)_6$. As with $Ru(NH_3)_6Cl_2$, the crystal structure of the mixed salt $LaKRu(CN)_6 \cdot 4H_2O$ reveals that ruthenium is at a site of octahedral symmetry. The compound crystallizes in the hexagonal space group $P6_3/m$ with four water molecules.[46] The solid-state ^{99}Ru NMR spectrum of $LaKRu(CN)_6 \cdot 4H_2O$, acquired under MAS conditions at 11.75 T, shown in Figure 1b, consists of a broad peak, $\delta_{iso} = -247 \pm 2$ ppm with $\Delta\nu_{1/2} = 530$ Hz. This peak may consist of several overlapping peaks originating from various hydrates; $LaKRu(CN)_6 \cdot xH_2O$ ($x \leq 4$) produced as a result of heating from rapid magic-angle spinning (vide infra).

The ^{99}Ru NMR spectrum for $K_4Ru(CN)_6$ acquired under MAS conditions consists of two isotropic ($^1/_2 \leftrightarrow -^1/_2$) peaks at 17 ± 1 ppm and -14 ± 1 ppm (an expansion of the centerband region is presented in Figure 1c). In this case, spinning sidebands (ssb) from the $\pm^3/_2 \leftrightarrow \pm^1/_2$ and $\pm^5/_2 \leftrightarrow \pm^3/_2$ satellite transitions are also observed (see Figure 2). Unlike the LaK salt, X-ray crystallography reveals that the ruthenium nucleus in the potassium salt $K_4Ru(CN)_6 \cdot 3H_2O$ does not reside in a site of octahedral symmetry.[71] The structure at room temperature, which is isostructural with $K_4Fe(CN)_6 \cdot 3H_2O$,[72] has four unique cyanide ligands, two unique potassium ions, and two unique water molecules. Thus, on the basis of the crystal structure, the EFG at ruthenium and the magnetic shielding anisotropy are expected to be small but nonzero. The crystal structure of $K_4Ru(CN)_6 \cdot 3H_2O$ also indicates that there is only one unique ruthenium atom per unit cell.[71] The presence of two peaks suggests that two structural forms of the hexacyanoruthenate are present in the sample. The sample was placed in an oven at 140 °C for 24 h, and the spectrum that was subsequently acquired contained only the peak at 17 ± 1 ppm. Since the trihydrate salt loses all three water molecules by 140 °C, as determined by thermal gravimetric analysis, we attribute the peak at 17 ± 1 ppm to an anhydrous salt, $K_4Ru(CN)_6$, whereas the peak at -14 ± 1 ppm is attributed to the trihydrate salt. In an attempt to acquire a spectrum of the pure hydrate salt, the sample was dissolved in water and allowed to air-dry overnight, after which the sample was packed into an airtight rotor. During the first few hours of data collection only the hydrate peak, $\delta_{iso} = -14 \pm 1$ ppm, was present; however, after approximately 6 h of sample spinning at 2.5 kHz, the peak at 17 ± 1 ppm began to appear. This observation suggests that the waters of hydration are being removed from the sample because of the heating caused by sample spinning.[73] There do not appear to be any intermediate forms of hydration between the trihydrate and anhydrous salts.

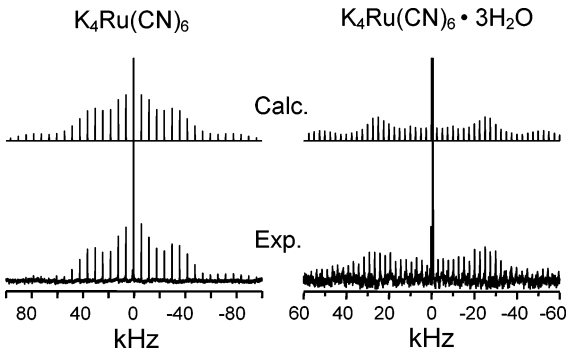

Figure 2. Experimental (bottom) ^{99}Ru NMR spectra of solid anhydrous $K_4Ru(CN)_6$ and $K_4Ru(CN)_6 \cdot 3H_2O$ acquired at 23.040 MHz (11.75 T) with MAS. Experimental spectra were acquired with a 0.5 s recycle delay, 12 k scans at a 6.5 kHz MAS rate for $K_4Ru(CN)_6$ and a 0.5 s recycle delay, and 29 k scans at a 2.5 kHz MAS rate for $K_4Ru(CN)_6 \cdot 3H_2O$. A small amount of anhydrous salt is also present in the hydrate sample. The calculated (top) spectra were calculated using the parameters presented in Table 1. Relative intensities of the outer peaks are reduced as a result of incomplete excitation due to the pulse width and probe Q.

Figure 2 shows that the ^{99}Ru NMR spectra of both the anhydrous and hydrate forms of $K_4Ru(CN)_6$ display significant ssb envelopes arising from first-order quadrupolar effects on the satellite transitions (i.e., $\pm^5/_2 \leftrightarrow \pm^3/_2$, $\pm^3/_2 \leftrightarrow \pm^1/_2$). By simulating these ssb envelopes, the quadrupolar parameters can be determined.[42] The individual ssb's do not exhibit line shapes characteristic of second-order quadrupolar effects, indicating that the C_Q values are small. The difference in quality between the two experimental ^{99}Ru NMR spectra (Figure 2) is a result of the lower spinning speed that was necessary to obtain a spectrum of the predominantly hydrated form. Nevertheless, the quadrupolar coupling constant and asymmetry parameter can be estimated, $C_Q = 0.40 \pm 0.05$ MHz and $\eta_Q = 0.1 \pm 0.1$ (Table 1). The ^{99}Ru NMR spectrum obtained for the anhydrous form is significantly higher in quality, and therefore the EFG parameters can be more confidently determined; $C_Q = 0.35 \pm 0.02$ MHz and $\eta_Q = 0.85 \pm 0.05$. For both the trihydrate and anhydrous salts there was no evidence of magnetic shielding anisotropy in the ^{99}Ru NMR spectra obtained for stationary samples (not shown).

The change in the ruthenium EFG upon dehydration of $K_4Ru(CN)_6 \cdot 3H_2O$ is significant. Of particular interest is the change in η_Q from near axial symmetry in the trihydrate form to 0.85 in the anhydrous form. The crystal structure of the trihydrate form suggests a qualitative reason for the near axial

(71) Pospelov, V. A.; Zhdanov, G. A. *Zh. Fiz. Khim.* **1947**, *21*, 405−410.
(72) Kiriyama, R.; Kiriyama, H.; Wada, K.; Niizeki, N.; Hirabayashi, H. *J. Phys. Soc. Jpn.* **1964**, *19*, 540−549.
(73) Vangorkom, L. C. M.; Hook, J. M.; Logan, M. B.; Hanna, J. V.; Wasylishen, R. E. *Magn. Reson. Chem.* **1995**, *33*, 791−795.

Table 2. Experimental and Calculated ^{99}Ru NMR Parameters Determined for $Ru_3(CO)_{12}$ and the Chemical Shift Reference, $K_4Ru(CN)_6$

	σ_{iso}/ppm	δ_{iso}/ppm[a]	Ω/ppm	κ	C_Q/MHz	η_Q	α, β, γ/deg
			Experimental				
$Ru_3(CO)_{12}$ site 1		−1312 ± 5	1375 ± 30	0.35 ± 0.12	1.60 ± 0.1	0.9 ± 0.1	0, 90, (0 or 90) ± 10
site 2		−1309 ± 5	1375 ± 30	0.30 ± 0.06	1.36 ± 0.1	0.8 ± 0.1	0, 90, (0 or 90) ± 5
site 3		−1285 ± 5	1340 ± 30	0.35 ± 0.06	1.85 ± 0.1	0.5 ± 0.1	0, 90, (0 or 90) ± 5
			Relativistic ZORA−TZ2P				
$Ru_3(CO)_{12}$ site 1	1027	−1195	1428	0.36	−3.9	0.13	0, 90, 150
site 2	1025	−1193	1472	0.33	−2.8	0.83	0, 90, 142
site 3	1003	−1171	1436	0.34	−2.3	0.53	0, 90, 142
$K_4Ru(CN)_6$	−168	0					
			Nonrelativistic B3LYP−DZVP				
$Ru_3(CO)_{12}$ site 1	834	−1413	1340	0.59	−5.0	0.43	0, 90, 0
site 2	839	−1418	1379	0.56	−3.9	0.78	0, 90, 0
site 3	822	−1401	1327	0.59	−3.4	0.72	0, 90, 0
$K_4Ru(CN)_6$	−579	0					

[a] The calculated magnetic shielding values were referenced to the calculated shielding value of a geometry-optimized structure of $K_4Ru(CN)_6$ taken from ref 24.

symmetry of the EFG tensor. While no obvious symmetry is present in the immediate coordination environment of ruthenium, i.e., the Ru−C bond lengths and C−Ru−C bond angles, long-range symmetry is evident. For the trihydrate salt, there is approximate C_4 symmetry about the crystallographic *b*-axis, with four potassium ions lying slightly out of the $Ru(CN)_4$ plane in the crystallographic *ac*-plane. This results in the components of the EFG in the *ac*-plane being similar. In contrast, the environment along the crystallographic *b*-axis is different from the *a*- or *c*-axis, with K^+ ions around one of the CN^- groups and water molecules around the other. This is expected to make the component of the EFG that is perpendicular to the *ac*-plane significantly different from the two in-plane components leading to near axial symmetry of the EFG tensor.

While a crystal structure of the anhydrous form could not be obtained, the loss of water is thought to cause rearrangement of the potassium ions, as evidenced by the shattering of single crystals of $K_4Ru(CN)_6 \cdot 3H_2O$ upon dehydration. This change in structure is reflected in the Ru EFG tensors observed for the two forms. The magnetic shielding interaction depends primarily on local environment, such as the Ru−C bond lengths, while the EFG at the ruthenium is more sensitive to long-range effects. The 31 ppm difference in the isotropic Ru chemical shifts upon dehydration is small considering the sensitivity of Ru to changes in the local environment, suggesting that there are no dramatic alterations in the local structure of the $Ru(CN)_6^{4-}$ anion.

(c) $Ru_3(CO)_{12}$. (i) Solid-State NMR Spectroscopy. Triruthenium dodecacarbonyl is the best known ruthenium carbonyl. The molecule consists of three ruthenium atoms bonded together in a trigonal plane. Each ruthenium is also bonded to four carbonyl ligands, two of which are perpendicular to the Ru_3 plane and two of which are in the Ru_3 plane. There is a great deal of interest in various ruthenium carbonyl compounds because of their catalytic properties and their use as models for surface catalysts.[2,74−77] The molecular structure and its influence on catalytic properties are important aspects of the application

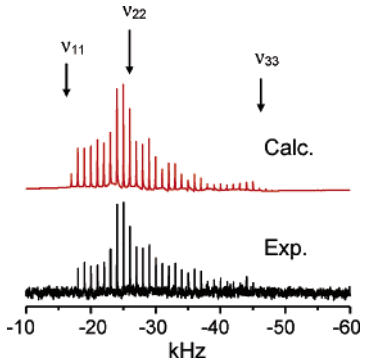

Figure 3. Experimental (bottom) solid-state ^{99}Ru NMR spectrum of the $^1/_2 \leftrightarrow -^1/_2$ transition of $Ru_3(CO)_{12}$ using the QCPMG pulse sequence on a stationary sample acquired at 23.040 MHz (11.75 T). Echo times of 128 μs and a 1 ms acquisition time per echo were used. The spectrum is the summation of 34 k scans. The calculated (top) spectrum was calculated using the parameters presented in Table 2. The ν_{ii} values correspond to the approximate positions of the principal components of the Ru magnetic shielding tensors, in frequency units: $\nu_{11} = -16.1$ kHz (−697 ppm), $\nu_{22} = -26.6$ kHz (−1156 ppm), $\nu_{33} = -47.2$ kHz (−2047 ppm).

of these metal-cluster systems. In the case of $Ru_3(CO)_{12}$, a structure from single-crystal X-ray diffraction was originally reported in 1968[78] and redetermined in 1977.[66] All three ruthenium atoms and 12 carbonyl groups are crystallographically unique.[66,78] Previous ^{13}C NMR studies of this compound in the solid state have shown that 11 of the 12 unique carbon sites can be resolved using MAS.[79,80]

The NMR spectra used to determine the ^{99}Ru NMR parameters for $Ru_3(CO)_{12}$ in the solid state are shown in Figures 3−6. By iteratively fitting simulated spectra to all of these experimental spectra, the NMR parameters given in Table 2 were obtained. Figure 3 shows the QCPMG ^{99}Ru NMR spectrum of a stationary sample of $Ru_3(CO)_{12}$ acquired at a magnetic field strength of 11.75 T, and Figure 4 shows the spectrum obtained under MAS conditions at the same field. When the two spectra are compared, it becomes clear that the ^{99}Ru NMR spectrum of solid $Ru_3(CO)_{12}$ is dominated by anisotropic magnetic shielding rather than the quadrupolar interaction, which is unusual for quadrupolar nuclei. This is evidenced by the observation that

(74) Muetterties, E. L.; Rhodin, T. N.; Band, E.; Brucker, C. F.; Pretzer, W. R. *Chem. Rev.* **1979**, *79*, 91−137.
(75) Kettle, S. F. A.; Boccaleri, E.; Diana, E.; Rossetti, R.; Stanghellini, P. L.; Iapalucci, M. C.; Longoni, G. *Inorg. Chem.* **2003**, *42*, 6314−6322.
(76) Asaumi, T.; Chatani, N.; Matsuo, T.; Kakiuchi, F.; Murai, S. *J. Org. Chem.* **2003**, *68*, 7538−7540.
(77) Kondo, T.; Kaneko, Y.; Taguchi, Y.; Nakamura, A.; Okada, T.; Shiotsuki, M.; Ura, Y.; Wada, K.; Mitsudo, T. *J. Am. Chem. Soc.* **2002**, *124*, 6824−6825.
(78) Mason, R.; Rae, A. I. M. *J. Chem. Soc. A* **1968**, 778−779.
(79) Aime, S.; Dastru, W.; Gobetto, R.; Krause, J.; Milone, L. *Organometallics* **1995**, *14*, 4435−4438.
(80) Walter, T. H.; Reven, L.; Oldfield, E. *J. Phys. Chem.* **1989**, *93*, 1320−1326.

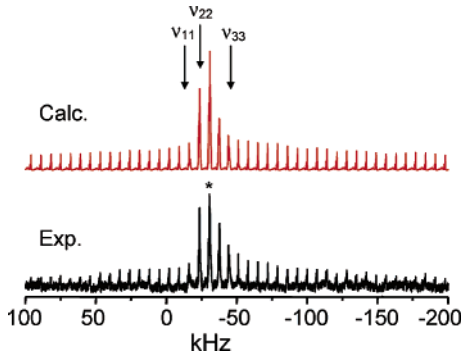

Figure 4. Experimental (bottom) solid-state ^{99}Ru NMR spectrum of $Ru_3(CO)_{12}$ using a recycle delay of 4 s at a 7.0 kHz MAS rate acquired at 23.040 MHz (11.75 T). The spectrum is the summation of 54 k scans. The asterisk denotes the position of the peaks invariant to the MAS rate. Ssb's from both the $+^1/_2 \leftrightarrow -^1/_2$ (between ν_{11} and ν_{33}) and $\pm^3/_2 \leftrightarrow \pm^1/_2$ transitions can be seen. Relative intensities of the outer peaks are reduced because of incomplete excitation due to pulse width and probe Q. The calculated (top) spectrum was obtained using the parameters presented in Table 2. The ν_{ii} values correspond to the approximate positions of the principal components of the Ru magnetic shielding tensors, in frequency units.

under conditions of MAS the central transition, $^1/_2 \leftrightarrow -^1/_2$, splits into relatively narrow (~2 kHz), distinct, ssb's (Figure 4); the MAS rate, 7.0 kHz, is much smaller than the span of the magnetic shielding tensor in frequency units. If the central-transition line shape of the stationary sample (breadth ≈ 35 kHz) was dominated by quadrupolar interactions, it would be impossible to obtain the observed sharp ssb's by spinning at 7.0 kHz.[42] The ^{99}Ru NMR spectra obtained at 17.6 T using three different spinning speeds (Figure 6) confirm that the ^{99}Ru C_Q values are small (<3 MHz) and that the span of the magnetic shielding tensor is greater than 1000 ppm.

From the QCPMG ^{99}Ru NMR spectrum (Figure 3) of a stationary sample of $Ru_3(CO)_{12}$, the presence of three magnetically distinct ruthenium sites is not apparent. This is not surprising because of the nature of the QCPMG experiment and the fact that the magnetic shielding tensors for the three ruthenium sites are not expected to be substantially different (vide infra). From the shape of the QCPMG spectrum it can be estimated that the spans, Ω, of the shielding tensors are between 1300 and 1400 ppm and the skews, κ, are between 0.2 and 0.5. The line shape of the QCPMG spectrum also places restraints on the three Euler angles (α, β, γ).[81] While a number of different orientations are compatible with the experimental spectra, the best results are obtained for the angles $\alpha = 0°$, $\beta = 90°$, and $\gamma = 0°$, which is consistent with the known structure about the ruthenium nuclei. On the basis of the local symmetry, one component of each tensor is expected to be perpendicular to the Ru_3 plane while the other two lie in the plane, with one bisecting the Ru−Ru−Ru bond angle; this assumption restricts the Euler angles to being either 0° or 90°. Of all possible combinations of these angles, only the set where $\alpha = 0°$, $\beta = 90°$, and $\gamma = 0°$ or 90° yields a line shape consistent with experiment. The orientation with $\gamma = 0°$ is in best agreement with the quantum chemical calculations, as shown in Table 2 (vide infra).

Since the ^{99}Ru C_Q values are small, they play a minor role in determining the breadth of the spectrum shown in Figure 3;

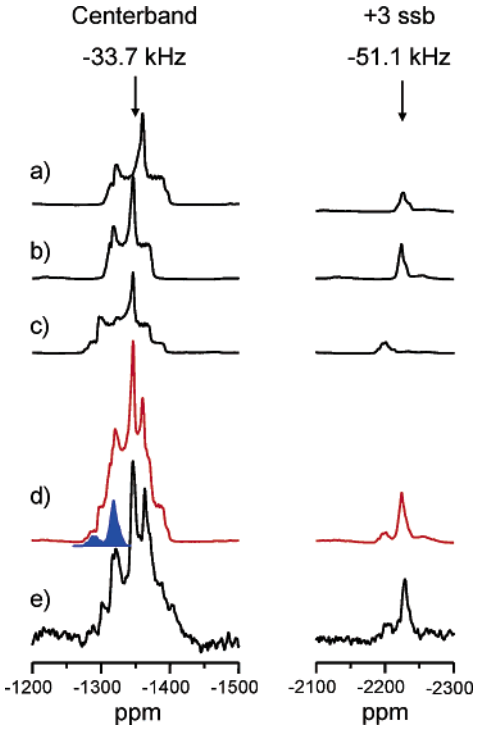

Figure 5. An expansion of the centerband region (−33.7 kHz) and the +3 ssb (−51.1 kHz) of solid $Ru_3(CO)_{12}$ under MAS conditions (7.0 kHz) at 11.75 T. (a−c) Individual site simulations for sites 1, 2, and 3, respectively. (d) Simulated spectrum of all three sites summed together. (e) Experimental spectrum. The parameters determined from the experimental spectrum are given in Table 2. The shaded peak shows the contribution that the $\pm^3/_2 \leftrightarrow \pm^1/_2$ satellite transition makes to the centerband region. The +3 ssb is solely from the $\pm^3/_2 \leftrightarrow \pm^1/_2$ satellite transitions.

however, both C_Q and η_Q influence the overall line shape of the spectrum. Given that $\alpha = 0°$, $\beta = 90°$, and assuming $\gamma = 0°$, the simulations indicate that the C_Q values must be less than 2.3 MHz. On the basis of numerous simulations, the asymmetry parameters for all three sites are ≥0.5 (vide infra).

To simulate the experimental ^{99}Ru NMR spectrum obtained with MAS at 11.75 T (Figure 4), it was necessary to include both anisotropic magnetic shielding and the quadrupolar interaction for each of the three sites. By comparing the breadth of the MAS spectrum to the stationary QCPMG spectrum collected at the same field strength (Figure 3), it is clear that the centerband and the +1, −1, and −2 ssb's contain significant contributions from anisotropic magnetic shielding as well as second-order quadrupolar interactions; the remaining ssb's arise from the $\pm^3/_2 \leftrightarrow \pm^1/_2$ satellites, as is verified by the fact that they are narrower than the central transition peaks by a factor of 0.29 (Figure 5).[82,83] The observation of an ssb pattern from the satellite transitions is another indication that the quadrupolar coupling constants are relatively small.[42] Ssb's from the $\pm^5/_2 \leftrightarrow \pm^3/_2$ satellite transition are expected to be broader than the central transition[82] and spread out over a larger frequency range, making them difficult to detect.

Figure 5e shows an expansion of the centerband and +3 ssb regions of the spectrum presented in Figure 4. The position of the centerband peaks (Figure 5e) does not vary as a function of spinning speed; their position is a result of the isotropic chemical

(81) Power, W. P.; Wasylishen, R. E.; Mooibroek, S.; Pettitt, B. A.; Danchura, W. *J. Phys. Chem.* **1990**, *94*, 591−598.
(82) Samoson, A. *Chem. Phys. Lett.* **1985**, *119*, 29−32.
(83) Samoson, A.; Lippmaa, E. *Chem. Phys. Lett.* **1983**, *100*, 205−208.

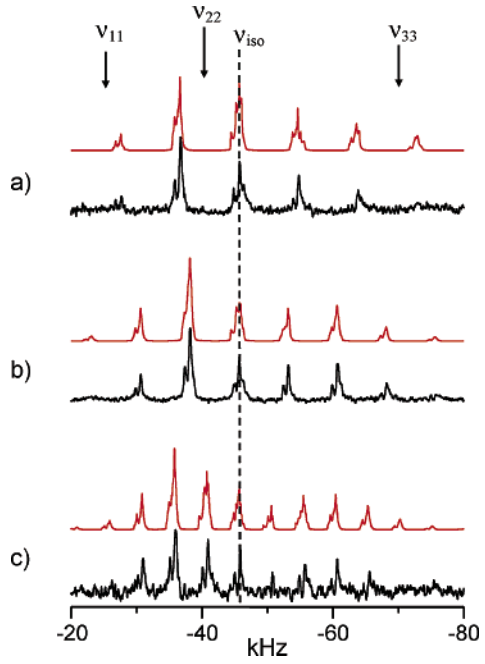

Figure 6. Experimental (bottom) solid-state ^{99}Ru NMR spectra of $Ru_3(CO)_{12}$ using a recycle delay of 2 s at: (a) 9.0 kHz, (b) 7.5 kHz, and (c) 5.0 kHz MAS rates acquired at 34.516 MHz (17.6 T). The spectra are the summation of 27 k, 64 k, and 25 k scans, respectively. The calculated (top) spectra were obtained using the parameters presented in Table 2. The ν_{ii} values correspond to the approximate positions of the principal components of the Ru magnetic shielding tensors, in frequency units: $\nu_{11} = -24.0$ kHz (-697 ppm), $\nu_{22} = -39.9$ kHz (-1156 ppm), $\nu_{33} = -70.7$ kHz (-2047 ppm).

shift and the second-order quadrupolar shift associated with a particular ruthenium site. The second-order quadrupolar shift is a consequence of the fact that the quadrupolar interaction has an isotropic component that is inseparable from the isotropic chemical shift.[82,84] As a result, the peaks from different transitions are shifted with respect to the isotropic chemical shift values by $\Delta\nu_{|m,m-1|}$ (in Hz):

$$\Delta\nu_{|m,m-1|} = -\frac{3}{40}\left(\frac{C_Q^2}{\nu_L}\right)\left(\frac{I(I+1) - 9m(m-1) - 3}{I^2(2I-1)^2}\right)\left(1 + \frac{\eta_Q^2}{3}\right) \quad (5)$$

where ν_L is the Larmor frequency of the nucleus, I is the nuclear spin quantum number, and m is $^1/_2$, $^3/_2$, or $^5/_2$, depending on the transition (i.e., $^1/_2$ for the central transition). To obtain accurate values of δ_{iso}, the C_Q and η_Q values must first be determined.

A number of general observations can be made by examining Figure 5. First, given that there are three ruthenium sites contributing to the centerband region, the peaks are relatively narrow, <150 ppm (3.45 kHz), again confirming that the second-order quadrupolar interactions, and thus C_Q values, are small. Second, one can determine that the three unique ruthenium sites have similar isotropic chemical shifts and quadrupolar coupling parameters. Figure 5a−c shows simulations of the three unique sites using the parameters presented in Table 2. The sum of these three spectra, shown in Figure 5d, is in good agreement with the experimental results (Figure 5e).

The key features that aid in the simulation of the three Ru sites are the general line shape and the presence of the satellite transition ssb's in Figures 4 and 5. The shoulders of the centerband peaks and the presence of sharp features in the centers (Figure 5) indicate that the η_Q values for the three sites are 0.5 or greater. The observation of the satellite transition ssb's in the 11.75 T spectrum allows one to refine the value of C_Q in the simulations (eq 5). Once values of C_Q and η_Q were estimated from analysis of the MAS spectra, the relative intensities of the ssb's were used to optimize Ω and κ for each of the three sites from the QCPMG spectrum (Figure 3).

Since the span of the magnetic shielding tensor in frequency units is directly proportional to the magnetic field strength while the second-order quadrupolar interaction is inversely proportional to magnetic field strength, acquiring spectra at two or more applied magnetic field strengths can help one separate these two interactions.[41−45] Thus, to confirm the accuracy of the results, spectra were acquired at 17.6 T using three MAS rates (Figure 6). The individual ssb's show significantly less fine structure at the higher magnetic field strength because of the inverse field dependence of the second-order quadrupolar interaction. On the basis of the position of the peaks using MAS rates of 5.0, 7.5, and 9.0 kHz, the δ_{iso} and C_Q values could be confirmed. The peaks between -1280 and -1360 ppm (i.e., -44.2 and -46.9 kHz) in the spectra collected at 17.6 T are independent of spinning speed. On the basis of the simulation of these spectra, the parameters determined from the spectra acquired at 11.75 T could be verified.

For $Ru_3(CO)_{12}$, the δ_{iso}, Ω, and κ values characterizing the three Ru magnetic shielding tensors are slightly different; however, experimental error prevents definitive conclusions about these differences. In contrast, the three C_Q values (1.60, 1.36, 1.85 MHz) differ beyond experimental error. The accuracy of the η_Q values (0.9, 0.8, 0.5) is somewhat limited by the quality of the MAS spectra; however, all three ^{99}Ru sites clearly have an η_Q greater than 0.4, and in the case of sites 1 and 2, the asymmetry parameter is close to 1. The large Ω values observed for the Ru nuclei of $Ru_3(CO)_{12}$ are not unexpected given that ruthenium has a chemical shift range of 18 000 ppm. On the other hand, the observation that the ^{99}Ru C_Q values are small is somewhat surprising given the lack of symmetry about the ruthenium nuclei. Nevertheless, on the basis of the narrow ^{99}Ru NMR peak width observed for $Ru_3(CO)_{12}$ in THF solution[22] and earlier DFT calculations,[24] the small C_Q values could have been anticipated.

(ii) DFT Calculations. Results of the ruthenium magnetic shielding calculations using the ZORA-DFT and B3LYP hybrid-DFT methods are presented in Table 2. Both computational methods yield excellent results for the Ω and δ_{iso} values. The differences in the calculated and experimental Ω and δ_{iso} values are less than 150 and 130 ppm, respectively. Given the large CS range for ruthenium, the small difference between experimental and calculated values may be fortuitous, especially for the B3LYP calculations where the basis set used for the ruthenium is small. Qualitatively, values of κ are also reproduced by both methods, with the ZORA-DFT calculation yielding superior results. Both computational methods indicate that Ω and κ for the three ruthenium sites do not differ dramatically; this prevents confident assignment of the NMR parameters determined experimentally to specific crystallographic ruthenium sites. The labeling of the three ruthenium sites used for the calculations presented in Table 2 correspond to that of the crystal

(84) Samoson, A.; Lippmaa, E. *Phys. Rev. B* **1983**, *28*, 6567−6570.

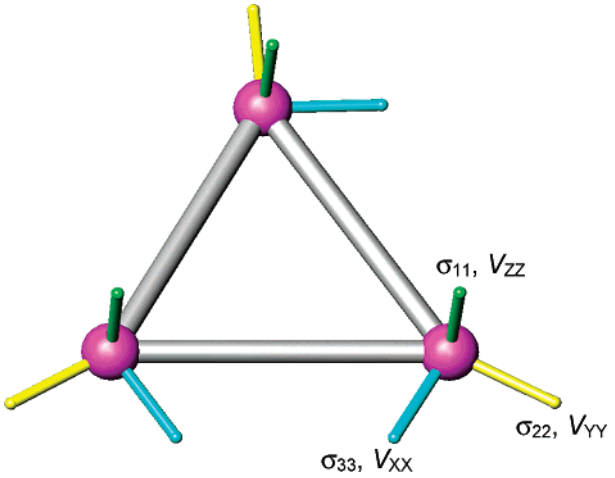

Figure 7. The orientation of the Ru magnetic shielding and EFG tensors for $Ru_3(CO)_{12}$ as predicted by the B3LYP calculation: σ_{11} and V_{ZZ} are perpendicular to the Ru_3 plane and σ_{22} and V_{YY} bisect the Ru−Ru−Ru bond angle. The same orientation of the shielding tensor was found using ZORA-DFT. The CO ligands have been omitted for clarity.

structure.[66] The orientation of the three Ru magnetic shielding tensors (Figure 7) is reproduced by both calculation methods; σ_{11} is perpendicular to the Ru_3 plane and σ_{22} bisects the Ru−Ru−Ru bond angle. Previous nonrelativistic DFT computations of ruthenium chemical shifts are in good agreement with isotropic values measured in solution;[24] our results further support this finding. Although the calculated magnetic shielding values obtained by relativistic and nonrelativistic methods differ substantially (see Table 2), the calculated chemical shifts are very similar. As more solid-state ^{99}Ru NMR data become available, the necessity of applying relativistic corrections to the calculation of magnetic shielding tensors for ruthenium and the use of larger basis sets can be further evaluated.

The ^{99}Ru EFG parameters were also calculated for $Ru_3(CO)_{12}$ using the ZORA-DFT and B3LYP computation methods (Table 2). Values obtained by the two methods are in qualitative agreement with experiment; however, both the ZORA-DFT and B3LYP calculations overestimate the C_Q values. For η_Q, the B3LYP method provides better agreement with values of 0.72, 0.78, and 0.43. The B3LYP calculation suggests that the EFG tensor is orientated such that V_{ZZ} is perpendicular to the Ru_3 plane and that V_{YY} bisects the Ru−Ru−Ru bond angle, thus the relative orientations of the magnetic shielding and EFG tensors are in agreement with experiment (Figure 7). The ZORA-DFT calculation yields slightly different orientations for the EFG tensors. For all three Ru nuclei, the V_{ZZ} component is predicted to be perpendicular to the Ru_3 plane, as with the B3LYP calculation, while V_{XX} and V_{YY} are rotated 30−40° away from the principal components of the shielding tensor, placing them closer to one of the Ru−Ru bonds for each of the three sites (see Table 2).

One probable source of error in the calculation of the EFG tensor is that only a single molecule was employed in the calculation. In a simple point-charge model, the EFG is proportional to $\langle r^{-3} \rangle$, where r is the point-charge to nucleus separation. Also, it is well-known that the calculation of EFG tensors for transition metals is difficult; for example, unreliable results have been previously reported using both the B3LYP and ZORA-DFT methods and have been attributed to deficiencies in the density functionals.[24,85−87] Previously, Bühl et al.[24] noted that B3LYP calculations of V_{ZZ} at the ruthenium nucleus of ruthenocene are approximately 60% greater than the experimental value. Given the difficulties in reproducing the experimental C_Q and η_Q values and the similarities in the three magnetic shielding tensors, it is impossible to make a definitive assignment of the NMR parameters to a particular crystallographic Ru site. We have tentatively assigned the Ru sites on the basis of the observed and calculated isotropic chemical shifts.

As previously mentioned, the small ^{99}Ru C_Q values determined experimentally for $Ru_3(CO)_{12}$ were unexpected given the apparent lack of symmetry at the ruthenium sites. By comparison, in hexagonally close-packed ruthenium metal, $C_Q \approx 2$ MHz.[39,40] While the B3LYP and ZORA-DFT methods are unsuccessful in quantitatively reproducing the observed EFGs at the ruthenium nuclei, they do qualitatively agree that the C_Q values are small.

Conclusions

Although solid-state ^{99}Ru NMR experiments are inherently challenging, we have demonstrated that such experiments are feasible for diamagnetic Ru(II) salts and $Ru_3(CO)_{12}$. By considering the geometry of the molecule and employing computational methods, useful information can be obtained. The large chemical shift range of ruthenium presents a wealth of opportunity to investigate the influence of small structural changes. For example, the sensitivity of ^{99}Ru chemical shifts to concentration and solvent effects was previously observed, and our results for $Ru(NH_3)_6Cl_2$ have also demonstrated that solid-state and solution chemical shifts are significantly different. Deviation from octahedral symmetry introduces an EFG at the Ru nucleus and possible anisotropic Ru magnetic shielding, as has been shown by comparing $LaKRu(CN)_6 \cdot 4H_2O$ and $K_4Ru(CN)_6 \cdot xH_2O$ ($x = 0, 3$). In the case of $Ru_3(CO)_{12}$, the stationary powder ^{99}Ru NMR line shape of the central transition is dominated by anisotropic magnetic shielding and not second-order quadrupolar broadening, an unusual result for a quadrupolar nucleus.

With the continued increase in magnetic field strengths, development of new spectrometer and probe hardware, and introduction of new pulse sequences, ^{99}Ru NMR will likely become a valuable tool for chemists. The ability to simultaneously characterize magnetic shielding and EFG tensors, both of which are sensitive to structure, has the potential to make ^{99}Ru NMR an important structural tool for anyone engaged in ruthenium chemistry.

Acknowledgment. We wish to thank the members of the solid-state NMR group at the University of Alberta for fruitful discussions. R.E.W. is a Canada Research Chair in Physical Chemistry at the University of Alberta and thanks the Natural Sciences and Engineering Research Council (NSERC) of Canada, the Alberta Ingenuity Fund, and the University of Alberta for research grants. K.J.O. thanks NSERC, the Alberta Ingenuity Fund, and the University of Alberta for post-graduate scholarships. Part of this research was performed at the

(85) Bast, R.; Schwerdtfeger, P. *J. Chem. Phys.* **2003**, *119*, 5988−5994.
(86) van Lenthe, E.; Jan Baerends, E. *J. Chem. Phys.* **2000**, *112*, 8279−8292.
(87) Schwerdtfeger, P.; Pernpointner, M.; Laerdahl, J. K. *J. Chem. Phys.* **1999**, *111*, 3357−3364.

Environmental Molecular Sciences Laboratory (a national scientific user facility sponsored by the U.S. DOE Office of Biological and Environmental Research) located at the Pacific Northwest National Laboratory, operated by Battelle for the DOE. We thank Nancy Isern, Dr. Andrew Lipton, Dr. Jesse Sears, and Dr. David Hoyt for their assistance with the 17.6 T NMR system and at PNNL; in particular, we are grateful to Dr. Jesse Sears for constructing the MAS probe for this narrow bore system. We acknowledge Prof. N. Chr. Nielsen and co-workers for making available the SIMPSON program. Finally, two anonymous reviewers are thanked for many helpful comments.

JA0400887